

Ultrafast spectral weight transfer in $R\text{BaCo}_2\text{O}_{6-\delta}$ ($R = \text{Sm, Gd, and Tb}$): Role of electronic correlation in a photoinduced phase transition

Y. Okimoto,¹ T. Miyata,¹ M. S. Endo,¹ M. Kurashima,¹ K. Onda,² T. Ishikawa,¹ S. Koshihara,^{1,3} M. Lorenc,⁴ E. Collet,⁴ H. Cailleau,⁴ and T. Arima⁵

¹*Department of Materials Science, Tokyo Institute of Technology, Meguro, Tokyo, 152-8551, Japan*

²*Department of Environmental Chemistry and Engineering, Tokyo Institute of Technology, Nagatsuta, Yokohama, 226-8503, Japan*

³*CREST, JST, Chiyoda-ku, Tokyo 102-0075, Japan*

⁴*Institut de Physique de Rennes, UMR 6251, CNRS-Universite, F-35042 Rennes Cedex, France*

⁵*Institute of Multidisciplinary Research for Advanced Materials, Tohoku University, Sendai 980-8577, Japan*

(Received 3 August 2011; published 30 September 2011)

We performed femtosecond reflection spectroscopy on a series of A-site ordered perovskite-type cobalt oxide $R\text{BaCo}_2\text{O}_{6-\delta}$ ($R = \text{Sm, Gd, and Tb}$) crystals, in which the electronic transfer was controlled by R . The transient reflectivity and the optical conductivity [$\sigma^{\text{PI}}(\omega)$] obtained by a Kramers-Kronig analysis showed an ultrafast change within a time resolution (≈ 150 fs) at room temperature and the appearance of signals of a hidden state that were different from the high-temperature metallic state. The transferred spectral weight in $\sigma^{\text{PI}}(\omega)$ upon photoexcitation sensitively depended on the R species, indicating an important role of electronic correlation in the photoexcited state.

DOI: [10.1103/PhysRevB.84.121102](https://doi.org/10.1103/PhysRevB.84.121102)

PACS number(s): 71.27.+a, 75.30.Wx, 78.47.jg

The photonic excited states in condensed matter have been extensively studied, stimulated by recent developments in laser technology. One of the most important and intriguing motivations in such studies is to actively create and control a unique phase concealed in the material by the irradiation of laser light. This is termed the photoinduced phase transition (PIPT) and has recently been noticed as an important research topic in nonequilibrium physics.¹ Several interesting examples using various optical techniques² have been demonstrated, especially in strongly correlated materials, which are subjected to external stimuli due to the close interaction between many degrees of freedom such as charge, spin, and lattice. In addition to experimental findings, theoretical approaches for elucidating the PIPT phenomena have been reported by exactly resolving the effective Hamiltonian in each target system.³

Among these approaches, spin-crossover (SC) Fe complexes are known as typical systems for the PIPT phenomena.⁴ This is a reversible photocontrol of the magnetic state of d electrons in the strong ligand field between two states: the low spin (LS) state (t_{2g}^6) stabilized by the crystal field and the high spin (HS) state ($t_{2g}^4 e_g^2$) by stabilized by Hund's coupling. In SC materials, the energy difference between the LS and HS states is so subtle that photoirradiation as well as temperature change can switch the spin configuration.

Another noted SC system is a class of perovskite-type cobalt oxide, and one such example is $\text{Pr}_{0.5}\text{Ca}_{0.5}\text{CoO}_3$ (PCCO), which undergoes a phase transition between the insulating LS state and the itinerant intermediate spin (IS) state ($t_{2g}^5 e_g^1$) in the Co^{3+} site.⁵ In this material, a photonic phase control in femtoseconds has been reported recently,⁶ which is an ultrafast insulator-metal (I-M) transition involved in the spin state transition between the LS and the IS state. This is in contrast to the simple magnetic PIPT observed in Fe complexes.⁴ This implies that the perovskite cobalt oxide systems containing trivalent Co ions offer us a unique arena for studying PIPT as a strongly correlated SC system.

From this point of view, a comparison with other cobaltite compounds $R\text{BaCo}_2\text{O}_{6-\delta}$ (RBCO, $R = \text{Sm, Gd, and Tb}$) can give important insight. The crystal structure of RBCO is shown in the inset of Fig. 1(a).⁷ The R -O and Ba-O layers are alternately stacked along the c axis, forming a quasi-two-dimensional (2D) structure. After annealing without any special condition, the δ value denoting oxygen deficiency was estimated as ≈ 0.5 . Hence, Co ions are almost trivalent (Co^{3+}). As seen in the schematics, there are two different Co sites, octahedral and pyramidal sites. While the spin state of Co^{3+} in the pyramidal site is always in the IS state with a configuration of ($t_{2g}^5 e_g^1$) due to the anisotropic ligand field, a thermally induced spin state change from the LS to HS states occurs in the octahedral sites above room temperature.⁸ In Fig. 1(b), we show the temperature dependence of resistivity (ρ) in $R = \text{Tb, Gd, and Sm}$. In the three materials, the ρ - T curves show a sudden jump⁹ at $T_{\text{IM}} \approx 350$ K, indicating an I-M transition.¹⁰ Upon the I-M transition, volume expansion occurs at T_{IM} , driven by spin excitation from the LS ground state,⁸ a characteristic feature of the SC system.

We performed time-resolved reflection spectroscopy on a series of RBCO ($R = \text{Sm, Gd, and Tb}$) crystals using a femtosecond laser system and we investigated the ultrafast dynamics in the photoexcited state at room temperature. There were two purposes of this study: One was to understand the electronic structure in the photoexcited as well as the thermally induced metallic states in the cobalt oxide, and the other was to systematically reveal the effect of electronic correlation on the appearance of the photoexcited state by changing the R site in RBCO crystals, in terms of an experimental point of view.

Single crystals of RBCO were grown using a floating-zone method.¹¹ The reflectivity spectrum [$R(\omega)$] for the light polarization perpendicular to the c axis was measured using a Fourier transform-type interferometer (0.01–0.7 eV) and grating monochromator (0.6–5 eV). The relative change in reflectivity ($\Delta R/R$) after photoirradiation was obtained with

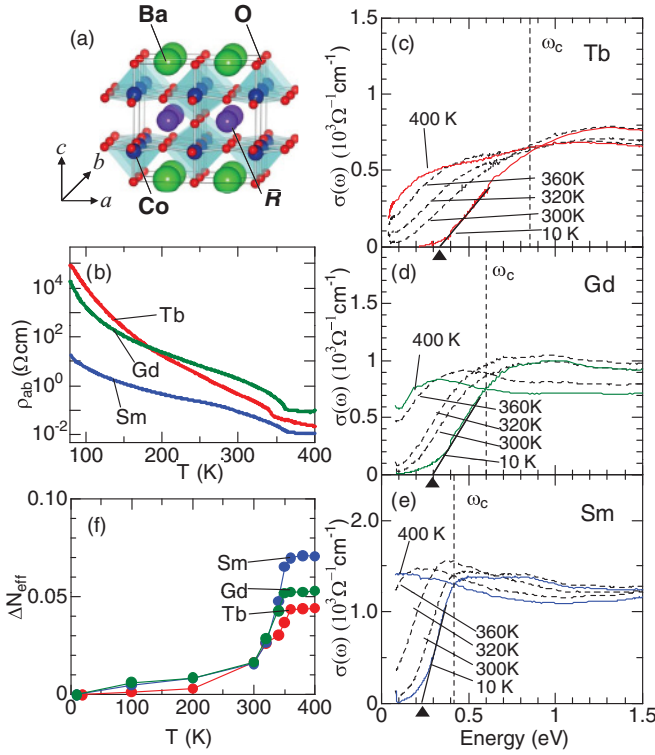


FIG. 1. (Color online) (a) Schematic drawing of the crystal structure in $\text{GdBaCo}_2\text{O}_{6-\delta}$ after Ref. 7. (b) Temperature dependence of resistivity (ρ) in $\text{RBaCo}_2\text{O}_{6-\delta}$ ($R = \text{Sm, Gd, and Tb}$). (c)–(e) Temperature dependence of optical conductivity [$\sigma(\omega)$] in $\text{RBaCo}_2\text{O}_{6-\delta}$ for $R = \text{Tb}$ (c), Gd (d), and Sm (e). (f) Temperature dependence of Drude weight D calculated from $\sigma(\omega)$ in $\text{RBaCo}_2\text{O}_{6-\delta}$.

the conventional pump-probe method using a Ti:sapphire regenerative amplifier system (pulse width ≈ 150 fs, repetition rate 1 kHz, and photon energy 1.58 eV) as a light source. The amplified light was separated into two light beams. We used one beam as a pump light for excitation. The photon energy of a pump light (1.58 eV) corresponds to the excitation energy from the O $2p$ to Co e_g bands.¹¹ The other beam, whose frequency was converted with an optical parametric amplifier, was used as a probe light to investigate transient $R(\omega)$ after photoexcitation from 0.12 to 2.1 eV. In all the ultrafast measurements, the polarization of the pump pulse was parallel to that of the probe pulse, and perpendicular to the c axis.

First and foremost, we discuss the role of R in the electronic structure. In the three-dimensional perovskite-type structure, the reduction of the ionic size of R generally brings about the lattice distortion and the resultant suppression of electron transfer (t),¹² and this can also be expected in a layered RBCO structure. Such an effect of the R size on the electronic structure in RBCO was confirmed using optical spectroscopy. Figures 1(c)–1(e) show temperature dependence of the optical conductivity spectra [$\sigma(\omega)$] in $R = \text{Sm, Gd, and Tb}$ crystals. At 10 K, all the spectral shapes of $\sigma(\omega)$ are gaplike, reflecting the insulating ground state. We estimated the optical gap (Δ_g) by linear extrapolation from the rising part of the $\sigma(\omega)$ to the abscissa, as shown by the solid lines and triangles. The evaluated values are listed in Table I with the ionic radii of R^{3+}

TABLE I. Physical parameters for $\text{RBaCo}_2\text{O}_{6-\delta}$.

R^{3+}	Sm	Gd	Tb
Ionic radius (Å)	1.240	1.215	1.203
Cutoff energy (eV)	0.36	0.52	0.80
Penetration depth (Å)	470	600	700
Optical gap (eV)	0.23	0.30	0.34

after the literature by Shannon.¹³ The value of Δ_g becomes large with decreasing ionic radius.

With increasing temperature, in all three samples, the onset energy of the absorption shows a gradual redshift, and finally a Drudelike metallic spectrum appears at 400 K above T_{IM} . To see the thermal spectral weight transfer more quantitatively, we have calculated the effective number of electrons (N_{eff}), defined as

$$N_{\text{eff}} = \frac{2m_0}{\pi e^2 N} \int_0^{\omega_c} \sigma(\omega) d\omega, \quad (1)$$

where m_0 and e are the mass and charge of an electron, respectively, and N is the number of Co ions in unit volume. For estimating the contribution from the inner gap excitation (i.e., Drude weight), we defined the cutoff energy (ω_c) as the crossing point in $\sigma(\omega)$ spectra at 10 and 400 K, as shown in Figs. 1(c)–1(e), and calculated D , the increased value in N_{eff} from the ground state with temperature [i.e., $D = N_{\text{eff}}(T) - N_{\text{eff}}(T = 10 \text{ K})$]. Figure 1(f) plots the temperature dependence of D . The value of D suddenly increases above T_{IM} , reflecting the I-M transition driven by the thermally excited e_g carriers. An important feature is that D in the metallic state strongly depends on the species of R . With decreasing the ionic size of R from $R = \text{Sm}$ to Tb , D decreases, indicating the suppression of the Drude weight due to the e_g carriers. The decrease in the ionic size brings about suppression of t for e_g electrons (t_A) through the lattice distortion, and hence it is reasonable to consider that D decreases with a decrease in the value of t_A . Hereafter, we demonstrate the results of femtosecond spectroscopy in the cobalt system and discuss the t_A dependence in the ultrafast dynamics by changing the species of R .

In the insets of Figs. 2(b)–2(d), we show the fluence dependence of $\Delta R/R$ at ≈ 0 ps in $R = \text{Sm, Gd, and Tb}$ at 0.75 eV.¹⁴ In all the samples, $\Delta R/R$ shows a gradual increase with increasing fluence. In some perovskite-type oxides,¹⁵ $\Delta R/R$ shows a thresholdlike fluence dependence. The observed results suggest that such threshold fluence, if any, is very small in the present cobalt system. With a further increase in the fluence, $\Delta R/R$ shows a saturation at around the excitation intensity (I_0), denoted by an arrow in each of these figures. This indicates that the photon number necessary for the complete photoinduced change becomes larger with decreasing t_A .

In Fig. 2(a), we show the time evolutions of $\Delta R/R$ at 0.5 eV in $R = \text{Sm, Gd, and Tb}$, with the pump fluence at I_0 . In all the samples, $\Delta R/R$ shows a sudden increase within the time resolution and the magnitude gradually decreases with an increase in t_A . Although some small decaying is observed, the photonically enhanced reflectivity seems to be kept up

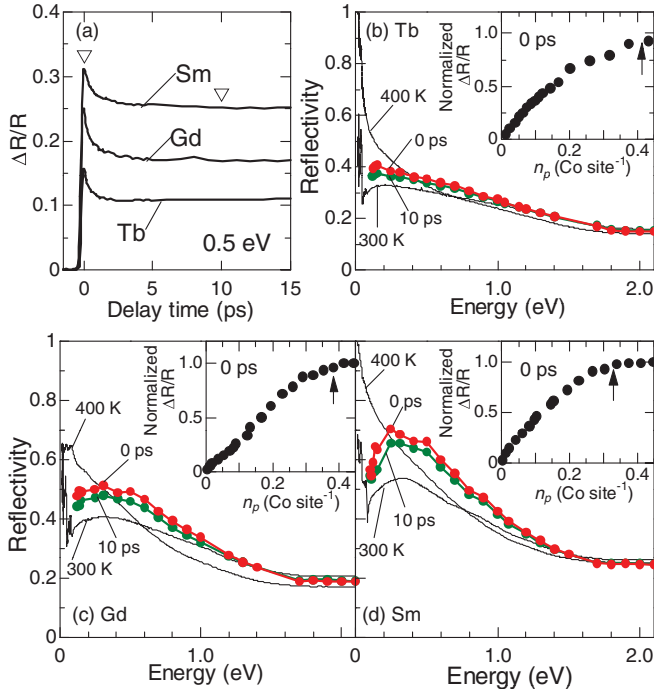


FIG. 2. (Color online) (a) Time profiles of $\Delta R/R$ at 0.5 eV for $R = \text{Tb}$, Gd, and Sm. (b)–(d) Transient reflectivity spectra just after (red/grayscale circles) and 10 ps after (green/dark gray circles) the photoirradiation in $\text{RBaCo}_2\text{O}_{6-\delta}$ for $R = \text{Tb}$ (b), Gd (c), and Sm (d). The solid lines show linear reflectivity spectra at 300 K (an insulating state) and 400 K (a metallic state). The insets show the fluence dependence of the relative change of reflectivity at 0.75 eV. The arrows denote means saturation fluence (I_0), and $I_0 = 7.4 \text{ mJ/cm}^2$ (Tb), $I_0 = 6.1 \text{ mJ/cm}^2$ (Gd), and $I_0 = 5.7 \text{ mJ/cm}^2$ (Sm).

to $\approx 1 \text{ ns}$, indicating a long lifetime and the stability of the photoinduced state, which is in contrast to the case of PCCO.¹⁶

Figures 2(b)–2(d) show the transient $R(\omega)$ spectra at $\approx 0 \text{ ps}$ (red/grayscale circles) and 10 ps (green/dark gray circles) in each sample, calculated from the $\Delta R/R$ with the fluence of I_0 at each delay time, as shown in the open triangles in Fig. 2(a). For reference, we also plot $R(\omega)$ in the equilibrium states at room temperature and 400 K, denoted by solid lines (the spiky structures below 0.1 eV are due to optical phonon modes). As the temperature increases, $R(\omega)$ at lower energies increases and a Drudelike spectrum appears in the metallic phase (400 K). As can be clearly seen, the spectral shapes of the transient $R(\omega)$ at $\approx 0 \text{ ps}$ are completely different from those at 400 K. This clearly indicates that simple heating by laser irradiation cannot explain the photoinduced reflectance change. Another important aspect is the degree of change in the transient $R(\omega)$ (ΔR) after photoirradiation. The ΔR value increases with an increase in t_A .

To see the t_A dependence in the optical spectra more clearly, we calculated the transient conductivity at $\approx 0 \text{ ps}$ [$\sigma^{\text{PI}}(\omega)$] by means of a Kramers-Kronig (K-K) analysis, considering the spatial variation of a dielectric function along the depth of the sample.¹⁸ We can numerically calculate the reflection phase change [$\theta(\omega)$] just after the photoexcitation from the transient $R(\omega)$ in Figs. 2(b)–2(d) in terms of the K-K analysis, extrapolating the constant reflection below 0.1 eV and $R(\omega)$

before the excitation above 2.1 eV. It is reasonable to consider that the yield of PIPT exponentially decreases along the distance from the surface (z) with a decrease in the pump light [see the inset of Fig. 3(c)]. Under these circumstances, the total dielectric constant [$\epsilon^{\text{crystal}}(z)$] after photoirradiation can be expressed by the following relation: $\epsilon^{\text{crystal}}(z) = \gamma \exp(-z/d)\epsilon^{\text{PI}} + [1 - \gamma \exp(-z/d)]\epsilon^{300 \text{ K}}$, where ϵ^{PI} and $\epsilon^{300 \text{ K}}$ are the dielectric functions just after and before the photoexcitation, respectively, and γ denotes the efficiency of the PIPT, which is fixed at 1, considering the photoexcitation just before the saturation in the fluence dependence. d is a penetration depth at 800 nm as listed in Table I. With these conditions, $R(\omega)$ and $\theta(\omega)$ can be described as a function of the real and imaginary part of ϵ^{PI} . By numerically solving these simultaneous equations, we can extract ϵ^{PI} from the obtained data.

In Figs. 3(a)–3(c), we show the calculated $\sigma^{\text{PI}}(\omega)$, defined as $\omega \text{Im}[\epsilon^{\text{PI}}]/4\pi$, in $R = \text{Sm}$, Gd, and Tb at $\approx 0 \text{ ps}$ (black circles), together with linear $\sigma(\omega)$ at 300 and 400 K. In all the materials at $\approx 0 \text{ ps}$, the spectral weight of $\sigma^{\text{PI}}(\omega)$ in the midinfrared region increases, forming a broad peak. Such a transient spectral shape is completely different from that in the metallic state, which strongly indicates that photoexcitation created a phase that cannot be observed by thermally induced I-M, in accordance with the spin state transition.

In SC Fe complexes, photoexcitation causes the spin state transition between the LS and HS states, and several theoretical

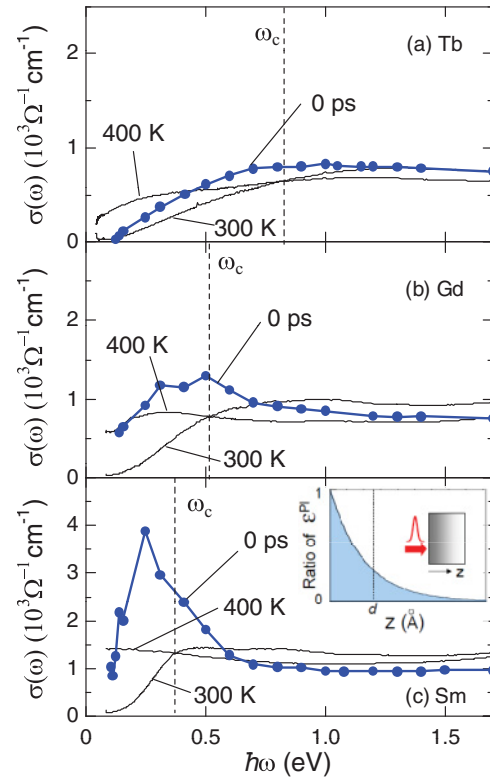


FIG. 3. (Color online) (a)–(c) Transient optical conductivity spectra [$\sigma^{\text{PI}}(\omega)$] just after the photoirradiation in $\text{RBaCo}_2\text{O}_{6-\delta}$ for $R = \text{Tb}$ (a), Gd (b), and Sm (c) (black circles). The solid lines show linear $\sigma(\omega)$ without photoirradiation at 300 and 400 K. The inset shows a schematic figure of the photoinduced state.

frameworks have been reported.⁴ However, in the present SC Co system, which shows a different phase from the high-temperature state, a different theoretical viewpoint regarding the strong correlation between e_g carriers is indispensable. Recently, Kanamori, Matsueda, and Ishihara have proposed an effective Hamiltonian to describe the spin state transition in a SC cobalt system using a two-band Hubbard model.¹⁹ They have numerically calculated the ground state after injecting a pair of electrons and holes in the effective Hamiltonian and revealed that the HS-hole bound state as a result of the photoexcitation was stabilized, which shows a nonmetallic absorption peak at $\omega \approx 2t_A$ in $\sigma^{\text{PI}}(\omega)$, with the Drude component due to the free electrons and holes in the lower-energy region. In the experiment, the peak position in Sm [Fig. 3(c)] is ≈ 0.3 eV, which corresponds to $2t_A$. Such a bound state, which is stabilized by the local double-exchange interaction, seems to be consistent with the observed photoinduced state having a clear midinfrared peak different from the Drude absorption.

It seems difficult to exactly estimate the peak position of $\sigma^{\text{PI}}(\omega)$ in $R = \text{Gd}$ and Tb , probably because of the weakness of the change, the strong absorption of the original charge-transfer transition, and the large spectral width of the absorption as observed in the case of $R = \text{Sm}$. Thus, we discuss the R dependence of the increased spectral weight just after photoirradiation (ΔN_{eff}), defined as

$$\Delta N_{\text{eff}} = \frac{2m_0}{\pi e^2 N} \int_0^{\omega_c} \sigma^{\text{PI}}(\omega) d\omega - N_{\text{eff}}(T = 300 \text{ K}). \quad (2)$$

We plotted ΔN_{eff} and D as a function of the ionic radius of R^{3+} ion in Fig. 4. By photoexcitation, ΔN_{eff} almost linearly increases with increasing the ionic size of R^{3+} , i.e., t_A , which strongly indicates that electronic correlation seriously affects the appearance not only of the thermally induced state but also of the photoinduced state. In addition, while the value of ΔN_{eff} is comparable to D in $R = \text{Tb}$, ΔN_{eff} becomes larger than D with further increasing t_A , indicating the larger spectral weight transfer by the photoexcitation than by the thermal change. It is worth noting here that the above-mentioned calculation¹⁹ also reproduces the two experimentally observed features; i.e., the photonically induced oscillator strength in $\sigma(\omega)$, which originated from the HS-hole bound state, increases with t_A , and

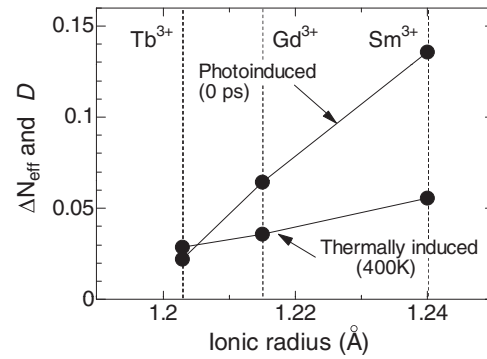


FIG. 4. The variation of the photoinduced (ΔN_{eff}) and thermally induced (D) spectral weight transfer as function of the ionic radius of R^{3+} in $\text{RBaCo}_2\text{O}_{6-\delta}$.

is larger than the thermally induced spectral weight, supporting the assignment of the midinfrared peak in $\sigma^{\text{PI}}(\omega)$.

In summary, we performed femtosecond reflection spectroscopy in perovskite-type cobalt oxide, where the electronic transfer t_A is controlled by changing the rare-earth species. The transient $R(\omega)$ as well as the calculated $\sigma^{\text{PI}}(\omega)$ showed an ultrafast change at room temperature, indicating (1) the appearance of a hidden state just after photoirradiation that is different from the high-temperature metallic state, which is assigned as the HS-hole bound state suggested by the recent theoretical calculation, and (2) that the transferred spectral weight by photoexcitation increases with increasing t_A , which is also consistent with theoretical prediction. These results indicate an important role of electronic correlation in the photoinduced phase transition, which not only sheds important insight on understanding the photoexcited state but also provides a good stage for exploring unique ultrafast nonequilibrium phenomena.

The authors thank T. Saito and K. Seko for technical assistance and Y. Kanamori, H. Matsueda, and S. Ishihara for fruitful discussions. This work was supported by Grant-in-Aid for Scientific Research on Innovative Areas (Grants No. 21104514) and G-COE in Tokyo Institute of Technology.

¹As a comprehensive review, see *Photoinduced Phase Transitions*, edited by K. Nasu (World Scientific, Singapore, 2004).

²A. Cavalleri, M. Rini, H. H. W. Chong, S. Fourmaux, T. E. Glover, P. A. Heimann, J. C. Kieffer, and R. W. Schoenlein, *Phys. Rev. Lett.* **95**, 067405 (2005); H. Okamoto, K. Ikegami, T. Wakabayashi, Y. Ishige, J. Togo, H. Kishida, and H. Matsuzaki, *ibid.* **96**, 037405 (2006); M. Chollet *et al.*, *Science* **307**, 86 (2005).

³For example, K. Yonemitsu and K. Nasu, *J. Phys.* **465**, 1 (2008); Y. Kanamori, H. Matsueda, and S. Ishihara, *Phys. Rev. Lett.* **103**, 267401 (2009).

⁴For example, *Spin Crossover in Transition Metal Compounds I, II and III*, edited by P. Gutlich and H. A. Goodwin (Springer, Berlin, 2004).

⁵S. Tsubouchi, T. Kyomen, M. Itoh, P. Ganguly, M. Oguni, Y. Shimojo, Y. Morii, and Y. Ishii, *Phys. Rev. B* **66**, 052418 (2002).

⁶Y. Okimoto, X. Peng, M. Tamura, T. Morita, K. Onda, T. Ishikawa, S. Koshihara, N. Todoroki, T. Kyomen, and M. Itoh, *Phys. Rev. Lett.* **103**, 027402 (2009); Y. Okimoto, M. Kurashima, K. Seko, T. Ishikawa, K. Onda, S. Koshihara, T. Kyomen, and M. Itoh, *Phys. Rev. B* **83**, 161101(R) (2011).

⁷Y. Moritomo, T. Akimoto, M. Takeo, A. Machida, E. Nishibori, M. Takata, M. Sakata, K. Ohoyama, and A. Nakamura, *Phys. Rev. B* **61**, 13325(R) (2000).

⁸C. Frontera, J. L. Garcia-Munoz, A. Llobet, and M. A. G. Aranda, *Phys. Rev. B* **65**, 180405(R) (2002); C. Frontera, J. L. Garcia-Munoz, A. E. Carrillo, M. A. G. Aranda, I. Margiolaki, and A. Caneiro, *ibid.* **74**, 054406 (2006).

- ⁹S. Roy *et al.*, *Phys. Rev. B* **65**, 064437 (2002); A. A. Taskin *et al.*, *ibid.* **71**, 134414 (2005).
- ¹⁰K. Takubo, J.-Y. Son, T. Mizokawa, M. Soda, and M. Sato, *Phys. Rev. B* **73**, 075102 (2006).
- ¹¹T. Saito, T. Arima, Y. Okimoto, and Y. Tokura, *J. Phys. Soc. Jpn.* **69**, 3525 (2000).
- ¹²J. B. Torrance, P. Lacorre, A. I. Nazzal, E. J. Ansaldo, and Ch. Niedermayer, *Phys. Rev. B* **45**, 8209 (1992).
- ¹³R. D. Shannon, *Acta Crystallogr. A* **32**, 751 (1976).
- ¹⁴We checked that $\Delta R/R$ hardly changed in a cross configuration of the polarization of the pump and probe light, excluding the so-called coherent artifact just after the photoexcitation.
- ¹⁵D. Fausti, Oleg V. Misochko, and Paul H. M. van Loosdrecht, *Phys. Rev. B* **80**, 161207(R) (2009); R. I. Tobey, D. Prabhakaran, A. T. Boothroyd, and A. Cavalleri, *Phys. Rev. Lett.* **101**, 197404 (2008).
- ¹⁶The crystal of PCCO is so soft that the electronic property can be changed by an ambient pressure of ≈ 10 bar (Ref. 17), signaling the shock wave induced by a laser pulse plays an important role in the propagation of the photoinduced state.
- ¹⁷T. Fujita *et al.*, *J. Phys. Soc. Jpn.* **73**, 1987 (2004).
- ¹⁸Y. Okimoto, H. Matsuzaki, Y. Tomioka, I. Kezsmarki, T. Ogasawara, M. Matsubara, H. Okamoto, and Y. Tokura, *J. Phys. Soc. Jpn.* **76**, 043702 (2007).
- ¹⁹Y. Kanamori, H. Matsueda, and S. Ishihara, *Phys. Rev. Lett.* (in press).